SPANDIDOS PUBLICATIONS

ONCOLOGY REPORTS 47: 49, 2022

Zinc finger protein 384 enhances colorectal cancer metastasis by upregulating MMP2

ZAIHUA YAN[1,2*], YU ZHOU[1,2*], YANG YANG[3*], CHONGPU ZENG[4], PEIDONG LI[1,2], HONGPENG TIAN[1,2], XUEGUI TANG[5] and GUANGJUN ZHANG[1,2]

[1]Second Department of Gastrointestinal Surgery; [2]Institute of Hepatobiliary, Pancreatic and Intestinal Disease, The Affiliated Hospital of North Sichuan Medical College, North Sichuan Medical College, Nanchong, Sichuan 637000; [3]Department of Dermatology, Xining First People's Hospital, Xining, Qinghai 810000; [4]Department of General Surgery, Wangcang County People's Hospital, Guangyuan, Sichuan 628200; [5]Anorectal Department of Integrated Traditional Chinese and Western Medicine, The Affiliated Hospital of North Sichuan Medical College, North Sichuan Medical College, Nanchong, Sichuan 637000, P.R. China

Received September 28, 2021; Accepted December 15, 2021

DOI: 10.3892/or.2022.8260

Abstract. Zinc finger proteins (ZNFs) serve key roles in tumor formation and progression; however, the functions and underlying mechanisms of dysregulated ZNF384 in colorectal cancer (CRC) are yet to be fully elucidated. Therefore, the present study initially aimed to investigate the expression levels of ZNF384 in CRC samples. Moreover, lentiviral ZNF384 overexpression and ZNF384 knockdown models were established in CRC cells. Transwell, wound healing and *in vivo* tail vein metastasis assays were carried out to evaluate the effects of ZNF384 on CRC cell metastasis. Furthermore, reverse transcription-quantitative PCR, western blotting, serial deletion, site-directed mutagenesis, dual-luciferase reporter and chromatin immunoprecipitation assays were conducted to investigate the potential underlying mechanisms. The results of the present study demonstrated that ZNF384 expression was markedly increased in CRC samples and this was associated with a poor prognosis. Notably, ZNF384 overexpression increased the levels of CRC cell invasion and migration, whereas ZNF384 knockdown inhibited CRC development. Moreover, the results of the present study demonstrated that ZNF384 mediated the expression of MMP2. MMP2 knockdown inhibited ZNF384-mediated CRC cell invasion and migration, whereas MMP2 overexpression ameliorated ZNF384 knockdown-induced inhibition of CRC progression. In addition, the results of the present study demonstrated that hypoxia-inducible factor 1α (HIF-1α) had the ability to bind to the ZNF384 promoter, thereby initiating ZNF384 expression. In human-derived CRC samples, the expression levels of ZNF384 were positively correlated with both MMP2 and HIF-1α expression. Collectively, these findings highlighted that ZNF384 may act as a prognostic marker and regulator of CRC metastasis.

Correspondence to: Dr Xuegui Tang, Anorectal Department of Integrated Traditional Chinese and Western Medicine, The Affiliated Hospital of North Sichuan Medical College, North Sichuan Medical College, 1 Maoyuan South Road, Nanchong, Sichuan 637000, P.R. China
E-mail: txg668nc@sohu.com

Dr Guangjun Zhang, Second Department of Gastrointestinal Surgery, The Affiliated Hospital of North Sichuan Medical College, North Sichuan Medical College, 1 Maoyuan South Road, Nanchong, Sichuan 637000, P.R. China
E-mail: zhanggj1977@126.com

[*]Contributed equally

Key words: colorectal cancer, zinc finger protein 384, MMP2, hypoxia-inducible factor 1α, migration, invasion

Introduction

In women and men, colorectal cancer (CRC) is the second and third most prevalent type of cancer, respectively (1). High CRC-associated mortality rates are attributed to the high levels of metastasis and recurrence (2). Advances in technological and genetic analyses have improved CRC diagnosis and therapy (3); however, the mortality rate of CRC remains at a high level (4). Further investigations into the underlying molecular mechanisms involved in CRC progression are required to identify potential prognostic markers.

The C2H2-type zinc finger protein (ZNF), which is encoded by the ZNF384 gene, is a transcription factor involved in the transcription of extracellular matrix genes (5). Coupling of ZNF384 with TET family genes, such as the TATA box binding protein-associated factor, transcription factor 3 and Ewing sarcoma breakpoint region 1 gene, serves vital roles in acute lymphocytic leukemia (6,7). Moreover, transactivating characteristics of the fusion protein have been reported in NIH3T3 cells, highlighting the oncogenic potential of ZNF384 as a fusion protein (8). In melanoma cells, ZNF384 overexpression was shown to promote metastasis (9). Although

previous studies have indicated that ZNF384 may act as an oncogenic factor that promotes cancer progression and metastasis, the specific expression levels and functions of ZNF384 in human CRC are yet to be fully elucidated.

The present study aimed to examine the expression levels of ZNF384 in CRC tissues and cells, and to determine its prognostic value in patients with CRC. Additionally, the effects of ZNF384 on CRC cell invasion and migration, as well as the underlying mechanism, were assessed.

Materials and methods

Cell culture. The normal colonic epithelial cell line FHC, 293T cells and six human CRC cell lines (SW480, Caco-2, SW620, HT29, LoVo and HCT116) were purchased from the American Type Culture Collection. The 293T and CRC cell lines were seeded in DMEM (Gibco; Thermo Fisher Scientific, Inc.) with 10% FBS (Gibco; Thermo Fisher Scientific, Inc.), and the FHC cell line was seeded in DMEM:F12 (cat. no. D8437; Sigma-Aldrich; Merck KGaA) with 10% FBS. Cells were incubated in a humidified atmosphere containing 5% CO_2 at 37˚C. For cell culture under 0.5% O_2 tension, the cells were incubated for 0-24 h in a humidified atmosphere at 37˚C in a multi-gas CO_2-O_2 incubator (NuAire) equilibrated with 0.5% O_2, 5% CO_2 and 94.5% N_2. The cell suppliers stated that the identity of the cells had been confirmed using STR profiling and were free of mycoplasma contamination. The HT29 cell line was also identified by STR profiling in the present study. The following STR profiling markers were analyzed: Amelogenin, CSF1P0, D3S1358, D2S1338, D5S818, D8S1179, D7S820, D13S317, D16S539, D19S433, D18S51, D21S11, Penta D, FGA, Penta E, TPOX, TH01 and vWA.

Patients and tissue samples. Between September 2008 and December 2009, CRC tissues and corresponding non-carcinoma samples (≥5 cm away from the tumor margin) were acquired from a total of 167 patients with CRC subjected to surgical resection at The Affiliated Hospital of North Sichuan Medical College (Nanchong, China). In addition, the metastatic lymph tissues were collected from 50 patients with lymph node metastasis. Three of the enrolled cases developed distant metastases and were subsequently excluded from the study. Prior to surgery, the enrolled patients did not receive any adjuvant therapies. Resected tissues were immersed in liquid nitrogen and stored at -80˚C for subsequent analyses. Ethics approval was obtained from the Medical Ethics Committee of North Sichuan Medical College [approval no. 2021ER(A)007]. Prior to study enrollment, patients provided written informed consent. In order to evaluate postoperative survival, all patients with CRC were periodically followed up for between 11 and 96 months. Table SI displays the clinical characteristics of the study participants.

Immunohistochemical (IHC) staining and evaluation. CRC tissues were collected from patients with CRC, fixed for 12 h in 4% paraformaldehyde at room temperature and subsequently embedded in paraffin. Samples were sectioned into 4-μm slices. After incubation for 2 h at 60˚C in an incubator, the sections were deparaffinized using dimethylbenzene and rehydrated using a descending alcohol series. Sections were subsequently incubated for 30 min at room temperature in the presence of 0.3% hydrogen peroxide, and blocked for 1 h using 10% BSA (Sangon Biotech Co., Ltd.) at room temperature. Sections were incubated overnight at 4˚C with the following antibodies: Rabbit anti-ZNF384 (1:50; cat. no. ab251673; Abcam), rabbit anti-HIF-1α (1:100; cat. no. ab243860; Abcam) and rabbit anti-MMP2 (1:100; cat. no. ab235167; Abcam). Subsequently, sections were incubated with an HRP-conjugated secondary antibody (1:200; Goat Anti-Rabbit IgG H&L; cat. no. ab205718; Abcam) at 37˚C for 2 h. The tissues were then stained at room temperature for 1 h using DAB (OriGene Technologies, Inc.) and counterstained for 1 min at room temperature using hematoxylin. All sections were dehydrated and sealed. Visualization and imaging were carried out using a light microscope (Carl Zeiss AG), and sections incubated with Rabbit IgG (1:50; cat. no. A7016; Beyotime Institute of Biotechnology) acted as negative controls (NCs). Scoring was based on the ratio of positively stained cells, namely: 0, 0-5; 1, 6-35; 2, 36-70; and 3, >70%. Staining intensities were as follows: 3, strong; 2, moderate; 1, weak and 0, no staining. Final score determination was carried out by multiplying the scores of the percentage of positive cells with those of the staining intensities. Final scores were defined as: -, 0-1; +, 2-3; ++, 4-6; and +++, >6. Low expression levels were determined by a total score <4, whereas elevated expression was defined as a total score ≥4. Two pathologists independently performed the scoring.

Establishment of lentiviruses and stable cell lines. The pLKO.1-EGFP-PURO (cat. no. FH1717; Hunan Fenghui Biotechnology Co., Ltd.) vector was used to establish lentiviral vectors with short hairpin (sh)RNA sequences, which were designated LV-shZNF384, LV-shHIF-1α, LV-shMMP2 and LV-shcontrol. The LV-shcontrol contained a non-targeting shRNA control. All shRNA sequences are displayed in Table SII. Lentiviral vectors with human ZNF384, MMP2 and HIF-1α gene sequences were established in PLVX-EGFP-IRES-PURO (cat. no. BR684; Hunan Fenghui Biotechnology Co., Ltd) and designated as LV-ZNF384, LV-MMP2 and LV-HIF-1α. An empty vector was used as the NC and labeled LV-control.

To generate stable cell lines, the pPACKH1 HIV Lentivector Packaging kit (Systems Bioscience, LLC) was used. Briefly, the expression plasmids, including control plasmids (1.0 μg) and pPACKH1 packaging plasmid mix [5.0 μg; pPACKH1-GAG (3.0 μg), pPACKH1-REV (1.0 μg) and pVSV-G (1.0 μg) plasmids; 3rd generation packaging system] were transfected into 293T cells at 37˚C using Lipofectamine® 3000 reagent (Invitrogen; Thermo Fisher Scientific, Inc.). After 24 h, the culture medium was mixed with 20% of the medium volume of PEG-it Reagent (Systems Biosciences, LLC), and incubated overnight at 4˚C. After centrifugation at 72,000 x g for 120 min at 4˚C, pellets were washed in 1X PBS and aliquots were stored at -80˚C. The viruses were transduced into SW480, Caco-2, SW620 and LoVo cells ($1x10^5$ cells/well) using polybrene (8 mg/ml; Sigma-Aldrich; Merck KGaA) with infection multiplicities of 30-50. After 24 h at 37˚C, fresh medium was used to replace the viral medium. Selection of stably transduced cells was carried out by the addition of puromycin (6 μg/ml) and the maintenance concentration of puromycin used was 3 μg/ml.

Western blotting and reverse transcription-quantitative (RT-q) PCR were used to confirm successful transduction.

In vivo metastasis assay. A total of 80 BALB/C nude female mice (age, 6 weeks; weight ~20 g) were purchased from Shanghai SLAC Laboratory Animal Co., Ltd. Animals were housed in a 60% humidified atmosphere at 24˚C, under a 12-h light/dark cycle with free access to purified drinking water and food. The Experimental Animal Ethics Committee of North Sichuan Medical College approved the present study (approval no. 20200908). For the *in vivo* tail vein metastasis assay, mice (n=10/group) were inoculated with $5x10^6$ cells in 100 μl PBS through the tail vein. The mice were divided in to the following groups: SW480 (LV-Control and LV-ZNF384), SW620 (LV-shControl and LV-shZNF384), SW480-ZNF384 (LV-shControl and LV-shMMP2) and SW620-shZNF384 (LV-Control and LV-MMP2). Mice survival was recorded daily for 9 weeks, after which, animals were sacrificed to remove the lung tissues. Lung tissues were collected, fixed with 4% paraformaldehyde for 12 h at room temperature and embedded in paraffin for subsequent pathological examination. Paraffin-embedded tissues were sectioned into 4-μm slices. Mice were sacrificed via an intraperitoneal administration of sodium pentobarbital (200 mg/kg). Finally, a dissection microscope (SZX7; Olympus Corporation) was used to count the tumor metastases formed in the lungs.

Hematoxylin and eosin (H&E) staining. Lung tissues sections were de-paraffinized in two changes of xylene, followed by rehydration in two changes of absolute ethanol, and two changes of 95 and 70% ethanol. Tissue was washed briefly in deionized water and stained with Harris hematoxylin (Thermo Fisher Scientific, Inc.). Slides were then processed in 0.25% acid alcohol, blued in lithium carbonate and counterstained with eosin solution (Thermo Fisher Scientific, Inc.). Tissues were dehydrated in two changes of 95% and absolute ethanol, and cleared in xylene. Photomicrographs were captured using an Olympus BH-2 light microscope with DP70 camera operating with DPS-BSW v3.1 software (Olympus Corporation).

Chromatin immunoprecipitation (ChIP) assay. The ChIP assay was conducted using the Magna ChIP G Assay kit (MilliporeSigma) according to the manufacturer's protocol. Briefly, crosslinking of the transfected SW480 cells was carried out for 10 min using 1% formaldehyde at 37˚C, followed by quenching with glycine. Co-immunoprecipitation of bound DNA from sonicated (VCX750; Sonics & Materials, Inc.; frequency: 20 kHz; 25% power; 4.5S impact; 9S gap; 14 times in total) cell lysates (six rounds of 15 sec on, 90 sec off) was carried out following incubation with primary antibodies against HIF-1α (rabbit; 1:100; cat. no. 36169; Cell Signaling Technology, Inc.), ZNF384 (rabbit; 1:200; cat. no. ab251673; Abcam) and normal IgG (rabbit; 1:100; cat. no. 3900; Cell Signaling Technology, Inc.) overnight at 4˚C. Amplification of the corresponding promoter binding sites was carried out using PCR, and the corresponding primer sequences are displayed in Table SII. PCR was performed using Taq DNA polymerase (cat. no. EP0405; Thermo Fisher Scientific, Inc.) and a PCR system (Takara Biotechnology Co., Ltd.). The thermocycling conditions were as follows: Initial denaturation at 94˚C for 5 min; followed by 35 cycles at 94˚C for 40 sec, 60˚C for 30 sec and 72˚C for 60 sec, and a final extension step at 72˚C for 7 min. Experiments were carried out for three biological repeats.

Cell proliferation analysis. An MTT assay was performed to assess the levels of cell proliferation. Briefly, 100 μl transfected cells (SW480 or SW620; $5x10^3$ cells/well) were plated in 96-well plates. Following incubation for 24, 48, 72 or 96 h, 5 mg/ml MTT solution (20 μl) was added to each well and incubated for a further 4 h at 37˚C. Subsequently, the MTT solution was removed and 150 μl DMSO was added. Absorbance was measured at a wavelength of 490 nm using a SpectraMax M5 microplate reader (Molecular Devices, LLC). Five biological repeats were performed.

Transwell migration and invasion assays. Transwell inserts with polycarbonate membranes (pore size, 8.0 μm) were placed in 24-well plates. The invasion assay was performed after precoating the upper chamber with 50 μl Matrigel (Corning, Inc.) for 30 min at 37˚C, followed by overnight drying. For the migration and invasion assays, $1x10^4$ and $1x10^5$ cells, respectively, were seeded in the top chamber. Subsequently, complete medium (600 μl) was added to the lower chamber and incubated for 24 h. Cells on the upper surface were removed by swabbing. Cells on the lower surface were fixed in 10% formalin at 25˚C for 20 min, followed by staining with crystal violet (0.1%) at 25˚C for 5 min and counted using an inverted light microscope (magnification, x20; Olympus Corporation). Three biological repeats were performed.

Wound healing assay. Cells were plated into 6-well plates and cultured under standard conditions until 100% confluence was reached. Subsequently, a 1-ml pipette tip was used to scratch the cell monolayer to generate a linear cell wound and the floating cells were gently washed twice with DMEM. Cells were cultured at 37˚C in DMEM (containing 1% FBS) for 24 h. The cells migrating into the wounded areas were captured using a light microscope (magnification, x20) at 0 and 48 h. Wound healing was assessed using MShot Image Analysis System 1.3.10 (Guangzhou Mingmei Photoelectric Technology Co., Ltd.). Wound closure was assess using the following equation: Wound closure (%)=(area at T0-area at T48)/area at T0 x100. Three biological repeats were performed.

RT-qPCR. Total RNA was extracted from tissues and cells using TRIzol® reagent (Invitrogen; Thermo Fisher Scientific, Inc.). PrimeScript RT Reagent kit (Takara Bio, Inc.) was used for cDNA synthesis according to the manufacturer's protocol. To determine the mRNA expression levels of ZNF384 and MMP2, qPCR was performed using SYBR Premix Ex Taq II (Takara Bio, Inc.) on the ABI 7500 Real-Time PCR system (Applied Biosystems; Thermo Fisher Scientific, Inc.). The qPCR thermocycling conditions were as follows: 95˚C for 10 min; followed by 40 cycles at 95˚C for 30 sec, 60˚C for 30 sec and 72˚C for 30 sec; followed by a final extension step at 72˚C for 2 min. Samples without a cDNA template were used as the NC. Analysis of amplification curves was carried out using SDS 1.9.1 software (Applied Biosystems; Thermo Fisher Scientific, Inc.). The expression levels of target genes

in the cell lines were determined using the $2^{-\Delta\Delta Cq}$ method (10) using the following equations: $\Delta Cq=\Delta Cq^{target}-\Delta Cq^{GAPDH}$ and $\Delta\Delta Cq=\Delta Cq^{expression\ vector}-\Delta Cq^{control\ vector}$. Expression levels were normalized to matched control cells, which were set to 1.0. In clinical tissue samples, fold changes in expression levels of target genes were also determined using the $2^{-\Delta\Delta Cq}$ method, as per the following equations: $\Delta Cq=\Delta Cq^{target}-\Delta Cq^{GAPDH}$, and $\Delta\Delta Cq=\Delta Cq^{tumor}-\Delta Cq^{nontumor}$ or $\Delta\Delta Cq=\Delta Cq^{lymph\ node\ metastatic}-\Delta Cq^{nontumor}$. Expression levels were normalized to healthy colorectal tissues, which were also set to 1.0. Primer sequences are displayed in Table SII.

Western blotting. Total proteins were extracted from cells using RIPA lysis buffer (Beijing Solarbio Science & Technology Co., Ltd.) supplemented with proteinase inhibitors. The BCA method was used to assess protein concentrations. Proteins (50 μg/lane) were separated by SDS-PAGE on 10% gels and were subsequently transferred to PVDF membranes. After blocking for 1.5 h with 5% skim milk at room temperature, the membranes were incubated overnight at 4˚C in the presence of primary antibodies against ZNF384 (rabbit; 1:1,000; cat. no. ab251673; Abcam), MMP2 (rabbit; 1:1,000; cat. no. ab235167; Abcam), HIF-1α (rabbit; 1:2,000; cat. no. ab243860; Abcam) and the control β-actin (mouse; 1:500; cat. no. ab8226; Abcam). Subsequently, membranes were incubated with anti-rabbit (HRP-conjugated; 1:5,000; cat. no. sc-2357; Santa Cruz Biotechnology, Inc.) and anti-mouse (HRP-conjugated; 1:10,000; cat. no. sc-2005; Santa Cruz Biotechnology, Inc.) secondary antibodies for 1 h at 37˚C. Visualization of protein bands was carried out using electrochemiluminescence reagent (cat. no. WBKLS0500; MilliporeSigma). Semi-quantification of protein expression levels was carried out using ImageJ software (version 1.8.0; National Institutes of Health), with β-actin used as the loading control. Experiments were carried out for three biological repeats.

Plasmid construction. Plasmid vectors were established using standard procedures. Primers used in the present study are displayed in Table SII. PCR was used to amplify the ZNF384 promoter sequence (-1,996/+115) from human genomic DNA extracted from SW480 cells using a genomic DNA extraction kit (cat. no. ab156900; Abcam). PCR was performed using Takara LA Taq polymerase and PCR system (Takara Biotechnology Co., Ltd.). The thermocycling conditions were as follows: Initial denaturation at 94˚C for 5 min; followed by 35 cycles at 94˚C for 30 sec, 60˚C for 30 sec and 72˚C for 40 sec, and final extension at 72˚C for 5 min. This sequence is localized at the transcriptional start site position (-1,996/+115) in the 5'-flanking region of the human ZNF384 gene. Vector construction was carried out by integrating both forward and reverse primers in the 5'- and 3'-ends of KpnI and HindIII sites, respectively. Insertion of PCR products between the digested HindIII and KpnI sites of the pGL3-Basic vector (Promega Corporation) was performed. Moreover, the 5'-flanking region deletion mutants of the ZNF384 promoter [(-1,996/+115) ZNF384; (-1,752/+115) ZNF384; and (-317/+115) ZNF384] were established using the (-1,996/+115) ZNF384 vector as the template. Mutations in the HIF-1α-binding sites in the ZNF384 promoter were made using the QuikChange II Site-Directed Mutagenesis kit (Stratagene; Agilent Technologies, Inc.). Vector construction was verified using first DNA sequencing (Sangon Biotech Co., Ltd.) and HIF-1α promoter vectors were designed in the same way.

Transient transfection and luciferase assay. ZNF384 and HIF-1α expression plasmids were generated by cloning ZNF384 or HIF-1α DNA into pCMV-tag2A vectors (Agilent Technologies, Inc.). SW480 or SW620 cells were cultured in a 24-well plate at $1x10^5$ cells/well. After 12-24 h incubation, cells were co-transfected with expression plasmids [0.6 μg; pCMV-ZNF384, pCMV-HIF-1α or the control (pCMV-Tag)], reporter plasmids (0.18 μg) and pRL-TK plasmids (0.02 μg) (Promega Corporation) using Lipofectamine 3000 reagent. A total of 5 h post-transfection, cells were washed and placed in fresh medium containing 1% FBS for 48 h to recover. Cells were subsequently serum-starved for assaying. A Dual-Luciferase Assay kit (Promega Corporation) was used to detect luciferase activities according to the manufacturer's protocol. Lysed transfected cells were centrifuged at 72,000 x g for 120 min at 4˚C in Eppendorf microcentrifuge tubes. A Modulus™ TD20/20 luminometer (Turner Designs) was used to determine relative luciferase activities. Luciferase activity was normalized to *Renilla* luciferase activity. Three biological repeats were performed.

Bioinformatics analysis. UALCAN (11) (http://ualcan.path.uab.edu/) is an online interactive resource, which also provides easy access to publicly available cancer omics data [The Cancer Genome Atlas (TCGA), Metastasis 500, Clinical Proteomic Tumor Analysis Consortium (CPTAC) and Children's Brain Tumor Tissue Consortium]. UALCAN was used to determine the mRNA and protein expression levels of ZNF384 in primary colon adenocarcinoma cases using data obtained from TCGA and CPTAC. Gene Expression Profiling Interactive Analysis (GEPIA; http://gepia2.cancer-pku.cn; version, 2) is an open-access online tool for the interactive evaluation of RNA sequencing data from 9,736 tumors and 8,587 healthy samples in TCGA and Genotype-Tissue Expression programs (12). GEPIA2 was also used to evaluate the association between ZNF384 expression levels, and HIF-1α and MMP2 expression levels in colon or rectum adenocarcinoma. The University of California Santa Cruz (UCSC) Genome Browser (13) (http://genome.ucsc.edu) is a popular web-based tool for quickly displaying a requested portion of a genome at any scale, accompanied by a series of aligned annotation 'tracks'. UCSC Genome Browser was used to find the promoter sequence of MMP2 and ZNF384. JASPAR (14) website (https://jaspar.genereg.net/) was used to analyze the MMP2 and ZNF384 promoter (accessed on 10 October 2019). The relative profile score threshold was set at 85%. Data were output after calculation through the JASPAR website.

RT-PCR array. Total RNA was extracted from SW480-ZNF384 and SW480-Control cells using TRIzol according to the manufacturer's protocol and reverse transcribed to cDNA using PrimeScript RT Reagent kit (Takara Bio, Inc.) according to the manufacturer's protocol. Subsequently, RT-PCR was carried out using the Human Tumor Metastasis RT2 Profiler PCR array (SuperArray Bioscience) in an ABI PRISM7900

system (Applied Biosystems; Thermo Fisher Scientific, Inc.), according to the manufacturer's instructions. The PCR cycling conditions were set as follows: 95˚C for 5 min; followed by 40 cycles at 95˚C for 15 sec, 60˚C for 15 sec and 72˚C for 20 sec, and a final extension step at 72˚C for 5 min. The results were analyzed using the ΔΔCq method as aforementioned.

Statistical analysis. Continuous data are displayed as the mean ± standard deviation, and TCGA and CPTAC data are displayed as median and interquartile range. The χ^2 test was used to analyze categorical data. Comparison of means between and among groups was carried out using Student's t-tests and one-way ANOVA followed by Tukey's or Dunnett's post hoc tests, respectively. Comparison of means among 50 matched primary CRC, lymph node metastatic and healthy tissue samples was carried out using repeated measures ANOVA followed by Tukey's post hoc tests. Based on variables from univariate analyses, determination of independent factors influencing survival was carried out using the Cox proportional hazards model. Kaplan-Meier was used for survival analysis following surgery, and the log-rank test was performed for comparisons of survival outcomes. Correlations between ZNF384 and MMP2 or HIF-1α expression levels in CRC samples were assessed using Spearman's rank correlation analysis. SPSS software (version, 19; IBM Corp.) was used for statistical analyses, and GraphPad Prism (version, 9; GraphPad Software, Inc.) was used for graph preparation. $P<0.05$ was considered to indicate a statistically significant difference.

Results

ZNF384 expression is markedly increased in human CRC tissues. To explore the functions of ZNF384 in CRC development, the expression levels of ZNF384 in TCGA and CPTAC datasets were evaluated. Compared with in healthy tissues, ZNF384 expression levels were significantly elevated in colon adenocarcinoma tissues (Fig. 1A and D). TCGA samples were categorized into two groups: i) High expression (with TPM values above the upper quartile) and ii) Low/Medium expression (with TPM values below the upper quartile). The upper quartile of ZNF384 expression in TCGA samples was 36.407. Based on TCGA datasets, patients with elevated ZNF384 expression levels exhibited shorter overall survival outcomes compared with those with lower ZNF384 expression levels, implying that ZNF384 may be involved in CRC progression (Fig. 1F). The mRNA expression levels of ZNF384 were also measured in 50 matched primary CRC, lymph node metastatic and healthy tissue samples. The results shown in Fig. 1B demonstrated that compared with in matched healthy tissues, ZNF384 mRNA expression levels were markedly increased in primary CRC tissues. Moreover, compared with in primary CRC tissues, ZNF384 mRNA expression levels were markedly elevated in lymph node metastatic tissues. Consistent with the aforementioned findings, ZNF384 protein expression levels were markedly elevated in CRC tissues compared with in adjacent healthy tissues (Figs. 1C, E and S1A).

Subsequently, ZNF384 expression levels and the potential clinical significance were evaluated in a cohort of CRC tissues using IHC staining. Elevated ZNF384 expression levels were positively associated with poor tumor differentiation, high lymph node metastasis and an increased American Joint Committee on Cancer stage (15), and elevated ZNF384 expression levels were an independent risk factor for CRC progression (Tables I and II). Patients with high expression of ZNF384 exhibited markedly poor survival outcomes compared with patients with low expression of ZNF384 (Fig. 1G). In addition, patients with high expression of HIF-1α and MMP2 exhibited markedly poor survival outcomes compared with patients with low expression of HIF-1α and MMP2 (Fig. S2). These results suggested that ZNF384 expression levels were elevated in CRC and may be associated with poor prognostic outcomes.

ZNF384 enhances CRC cell invasion and metastasis. The results of the present study demonstrated that ZNF384 expression was closely associated with tumor metastasis. SW480 and SW620 represented cells with low and high metastatic ability, respectively, and ZNF384 was differentially expressed in these two cell lines (Fig. 1H and I). Therefore, the present study selected these two cell lines to study the effect of ZNF384 on the proliferation of colorectal cancer cells. Notably, ZNF384 expression exerted no significant effect on the proliferation of SW480 and SW620 CRC cells (Fig. S3). Thus, the effect of ZNF384 expression on the migratory and invasive capacity of CRC cells was investigated. Both the mRNA and protein expression levels of ZNF384 were measured in various CRC cell lines, including a normal colonic cell line (FHC), and cell sublines with weak metastatic ability (SW480, Caco-2, HCT116 and HT29) or strong metastatic ability (SW620 and LoVo). Consistent with the clinical findings, the expression levels of ZNF384 were significantly elevated in the six CRC cell lines compared with in the healthy colonic cell line (Figs. 1H, I and S1B). In the six CRC cell lines, ZNF384 expression was significantly elevated in metastatic CRC cells (LoVo and SW620) compared with in non-metastatic cell lines (SW480, Caco-2, HT29 and HCT116). In addition, the trend in HIF-1α expression in CRC cells under conditions of normoxia were inconsistent with the expression levels of ZNF384 and MMP2; under normoxic conditions, HIF-1α was highly expressed in HT29 and HCT116 cells, whereas ZNF384 and MMP2 were highly expressed in SW620 and LoVo cells (Figs. S4, S1O, S1P and 1I). These findings indicated that ZNF384 may have a vital role in CRC metastasis (Fig. 1H and I). Subsequently, four stable cell lines were used to investigate the role of ZNF384 in CRC progression (Figs. 2A-C, S1C and D). The levels of *in vitro* CRC cell migration and invasion were investigated using Transwell assays. The results displayed in Fig. 2D demonstrated that ZNF384 overexpression was associated with a high number of migrating and invading cells; however, ZNF384 knockdown led to a notable decrease in the levels of cell migration and invasion. These findings were consistent with those of the wound healing assays (Fig. S5). Therefore, the results of the present study highlighted that ZNF384 promoted CRC cell migration and invasion.

To further establish the role of ZNF384 in metastasis, nude mice were injected with either SW480-ZNF384 or SW620-shZNF384-1 cells, or the corresponding control cells. The results of the present study demonstrated that mice that had been injected with cells overexpressing ZNF384 exhibited

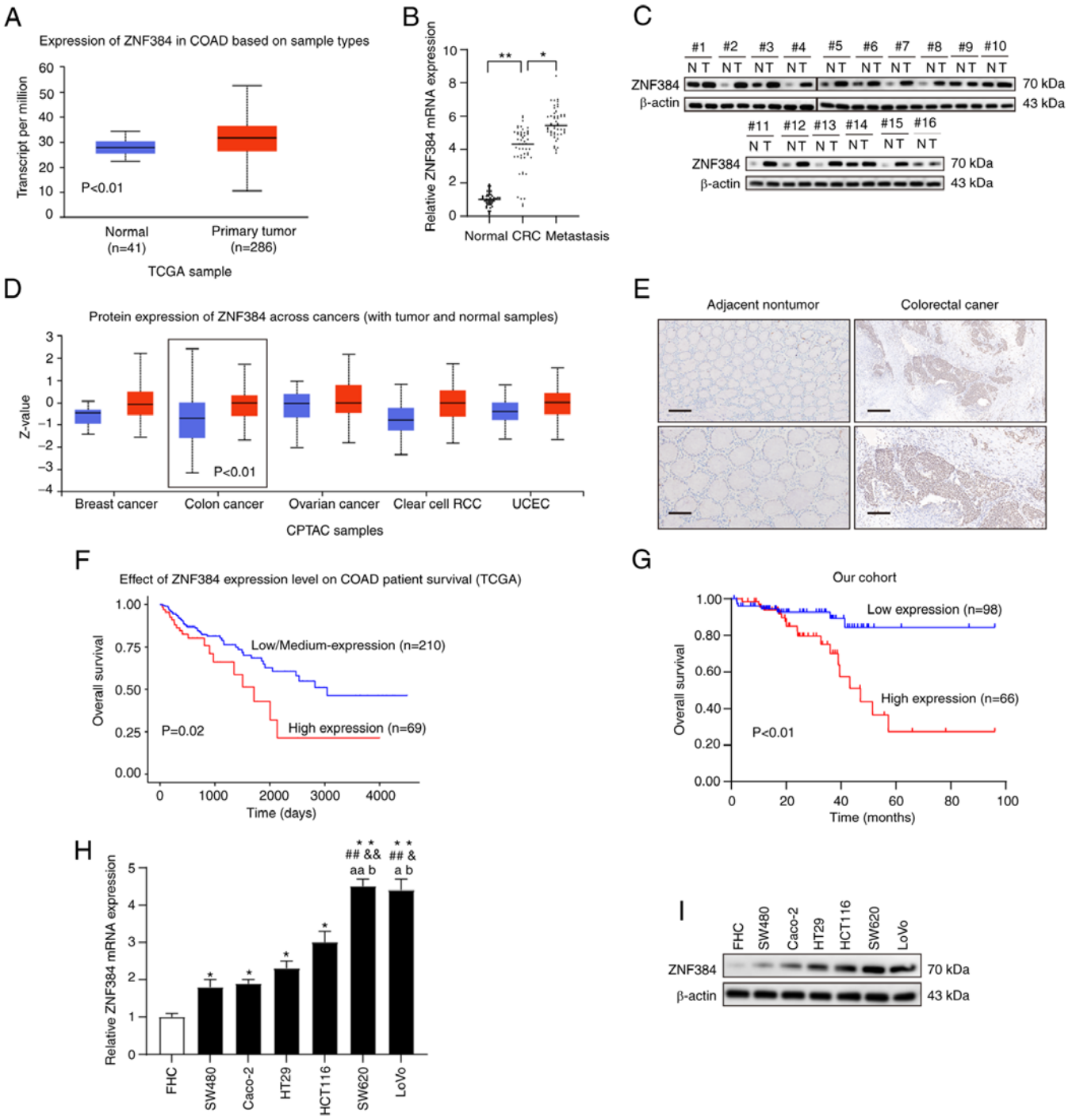

Figure 1. High levels of ZNF384 are predictors for poor prognostic outcomes in patients with CRC. (A) Representative data from TCGA datasets displaying the mRNA expression levels of ZNF384 in colon cancer tissues compared with in healthy tissues. Box-and-whisker plots represent medians (horizontal lines), interquartile ranges (boxes), and minimum and maximum values (whiskers). (B) mRNA expression levels of ZNF384 in normal, primary CRC and lymph node metastatic tissues. Expression levels of ZNF384 mRNA were determined by RT-qPCR and normalized to GAPDH. (C) Western blot analyses were conducted using human CRC and adjacent normal tissues. (D) ZNF384 protein expression levels in different tumor types and corresponding healthy tissues from UALCAN. (E) Immunohistochemical staining for the detection of ZNF384 in CRC tissues. Scale bars, 100 μm (upper panel) and 50 μm (lower panel). (F) Results of the Kaplan-Meier analysis demonstrated the association between ZNF384 mRNA expression levels and overall survival for patients with COAD in TCGA dataset. (G) Results of the Kaplan-Meier survival curves demonstrated the association between ZNF384 expression and overall survival outcomes in patients with CRC. (H and I) RT-qPCR and western blot analysis of ZNF384 expression levels in various CRC cell lines. *P<0.05, **P<0.01 vs. FHC; $^{\#\#}$P<0.01 vs. SW480; $^{\&}$P<0.05, $^{\&\&}$P<0.01 vs. Caco-2; ^{a}P<0.05, ^{aa}P<0.01 vs. HT29; ^{b}P<0.05 vs. HCT116. ZNF384, zinc finger protein 384; CRC, colorectal cancer; COAD, colon adenocarcinoma; N, normal; T, tumor; TCGA, The Cancer Genome Atlas; CPTAC, Clinical Proteomic Tumor Analysis Consortium; RT-qPCR, reverse transcription-quantitative PCR.

elevated CRC metastasis levels, whereas mice injected with cells in which ZNF384 was knocked down exhibited reduced CRC metastasis levels (Fig. 2E). In addition, the SW620-shControl group exhibited higher metastatic ability, compared with SW480-Control group. This is due to the difference in the metastatic ability of the two colorectal cancer

Table I. Associations between ZNF384 expression and clinicopathological parameters in 164 patients with colorectal cancer.

Clinicopathological variables	Number (n=164)	ZNF384 expression		P-value
		High (n=66)	Low (n=98)	
Age, years				0.101
<60	55	27	28	
≥60	109	39	70	
Sex				0.655
Male	83	32	51	
Female	81	34	47	
T stage				0.306
T1 and T2	57	26	31	
T3 and T4	107	40	67	
Lymphatic invasion				<0.01[a]
Absent	114	32	82	
Present	50	34	16	
AJCC stage				<0.01[a]
I	47	9	38	
II	67	27	40	
III	50	30	20	
Differentiation				0.016[b]
Well	35	15	20	
Moderate	73	21	52	
Poor	56	30	26	
Tumor location				0.651
Colon	76	32	44	
Rectum	88	34	54	

[a]P<0.01, [b]P<0.05. AJCC, American Joint Committee on Cancer.

cells themselves. Consistent with the aforementioned elevated lung metastasis levels, significantly reduced survival periods were observed in SW480-ZNF384 cell-injected mice compared with those injected with SW480-control cells (Fig. 2F). The survival period for SW620-shZNF384 cell-injected mice was significantly increased compared with the survival period of control cell-injected mice (Fig. 2F). Further histopathological evaluation of the lungs revealed a markedly high number of metastatic nodules in SW480-ZNF384-injected mice, compared with SW480-control-injected mice. Moreover, SW620-shZNF384 cell-injected mice exhibited significantly fewer metastatic nodules compared with those injected with SW620-sh control cells (Fig. 2G and H). In the tail vein metastasis assay, the nude mice quickly suffered casualties due to lung metastases, and colon metastases were rarely found. These results indicated that ZNF384 increased CRC cell invasion and metastasis.

MMP2 is a transcriptional target of ZNF384. To establish the mechanisms through which ZNF384 enhances CRC progression, a Metastasis RT2 Profiler PCR Array analysis was carried out to detect ZNF384 overexpression-associated transcriptomic variations in SW480 cells. By using a fold change of two as the cut off, 23 of the 89 metastasis-associated genes were elevated upon overexpression of ZNF384 in SW480 cells, 17 genes were suppressed and 49 genes did not exhibit any significant variations (Table SIII). Among the elevated genes, MMP2 had the strongest induction response to ZNF384 overexpression (Table SIII). Moreover, ZNF384, a transcriptional factor that exhibits a C2H2 ZNF structure, regulates MMP1, collagen α-1 chain precursor and MMP3 gene transcription levels (16-18). The transcriptional recognition site has an adenine enriched-sequence (15). By querying the UCSC Genome Browser, it was revealed that the promoter region of MMP2 is rich in adenine. Therefore, it was hypothesized that MMP2 was a target gene of ZNF384. To confirm whether ZNF384 activated MMP2 expression, the MMP2 mRNA and protein expression levels were evaluated in cells following either ZNF384 silencing or overexpression. ZNF384 overexpression significantly elevated the MMP2 mRNA expression levels, whereas the mRNA expression levels of MMP2 were markedly suppressed following ZNF384 knockdown (Fig. 3A and B). The changes in MMP2 protein expression levels were consistent with the aforementioned findings (Figs. 3C, S1E and F). To establish whether ZNF384 mediated MMP2 transcription activation, constructs expressing the MMP2 promoter were co-transfected with pCMV-ZNF384, and the relative luciferase activity was determined. The results

Table II. Univariate and multivariate analysis of factors associated with survival in patients with colorectal cancer.

Characteristics	Univariate analysis HR (95% CI)	P-value	Multivariate analysis HR (95% CI)	P-value
Age, years (≥60 vs. <60)	2.605 (0.9748-6.96)	0.056		
Sex (female vs. male)	0.986 (0.4466-2.179)	0.973		
T stage (T3 and T4 vs. T1 and T2)	1.114 (0.4691-2.647)	0.806		
Lymphatic invasion (present vs. absent)	5.931 (2.034-17.29)	0.001	3.849 (1.201-12.302)	0.022
Differentiation (poor vs. well/moderate)	1.817 (0.8395-3.934)	0.130		
AJCC stage (III vs. I and II)	3.088 (1.29-7.395)	0.010	0.998 (0.360-2.740)	0.897
Tumor location (colon vs. rectum)	0.995 (0.986-1.018)	0.549		
ZNF384 expression (high vs. low)	2.478 (1.102-5.574)	0.028	1.864 (1.450-2.380)	0.012
HIF-1α expression (high vs. low)	1.910 (1.020-3.575)	0.043	2.146 (0.881-5.230)	0.093
MMP2 expression (high vs. low)	3.946 (1.052-14.804)	0.042	3.472 (1.134-10.631)	0.029

AJCC, American Joint Committee on Cancer; HIF-1α, hypoxia-inducible factor-1α; ZNF384, zinc finger protein 384.

of the present study demonstrated that luciferase activity was markedly elevated in MMP2 promoter-transfected cells (Fig. 3D), indicating that ZNF384 activated MMP2 transcription. Moreover, sequence analysis via JASPAR revealed the presence of three putative ZNF384-binding sites in the MMP2 promoter. Site-directed mutagenesis and serial deletion analyses revealed that binding site 3 is vital for ZNF384-induced MMP2 transactivation (Fig. 3E). Furthermore, direct binding of ZNF384 to the MMP2 promoter was further verified using ChIP (Fig. 3F). These results indicated that ZNF384 directly binds to specific sites on the MMP2 promoter to transcriptionally activate subsequent gene expression.

MMP2 is crucial for ZNF384-mediated CRC cell migration and metastasis. Both MMP2 knockdown and overexpression were verified using RT-qPCR and western blotting (Figs. 4A-C, S1G-J, Q, R and S6). MMP2 knockdown significantly inhibited ZNF384-induced cell migration and invasion (Figs. 4D and S7); however, MMP2 overexpression reversed the ZNF384 knockdown-mediated levels of migration and invasion (Fig. 4E and S7). *In vivo,* the SW480-ZNF384 + LV-shMMP2-1 group exhibited poor metastasis, limited lung metastasis and scarce metastatic nodules, compared with the SW480-ZNF384 + LV-shControl group (Fig. 4F, I and J). However, MMP2 overexpression reversed the ZNF384 knockdown-induced decrease in SW620 cell metastasis (Fig. 4F, I and J). Compared with in mice injected with control cells, those that were injected with MMP2-overexpressing SW620-shZNF384 cells exhibited significantly reduced survival periods, whereas those injected with MMP2-knockdown SW480-ZNF384 cells exhibited significantly increased survival periods (Fig. 4G and H). These results indicated that ZNF384 may increase CRC migration and metastasis by promoting MMP2 expression.

HIF-1α transactivates ZNF384. Hypoxia is common in a number of malignancies, including CRC. Notably, the expression levels of HIF-1α and -2α have been reported to be elevated in numerous types of human cancer, and the expression levels of these proteins are associated with poor prognostic outcomes (19). The role of HIF-1α in cancer progression and the corresponding implications in CRC metastasis have previously been reported (20,21). During hypoxia, HIF-1α activates downstream genes involved in various cancer biological processes, such as angiogenesis, glucose metabolism, cell survival and invasion, to adapt to the hypoxic environment (22,23). Moreover, MMPs play important roles in this process, and a previous study indicated that HIF-1α initiated the expression of MMPs (24). Osinsky *et al* (25) demonstrated the positive correlation between hypoxia levels and MMP2, as well as MMP9, in Lewis lung carcinoma (25). Exposure of neonatal mice to chronic hypoxia (10% O_2), an inducer for lung development arrest, also led to elevated MMP2 levels with corresponding suppression of MMP inhibitor 2 precursor (26). Under hypoxic conditions (0.5% O_2), the ZNF384 expression levels in Caco-2 and SW480 cells were markedly elevated in a time-dependent manner (Figs. 5A, B, S1K and L). To investigate whether

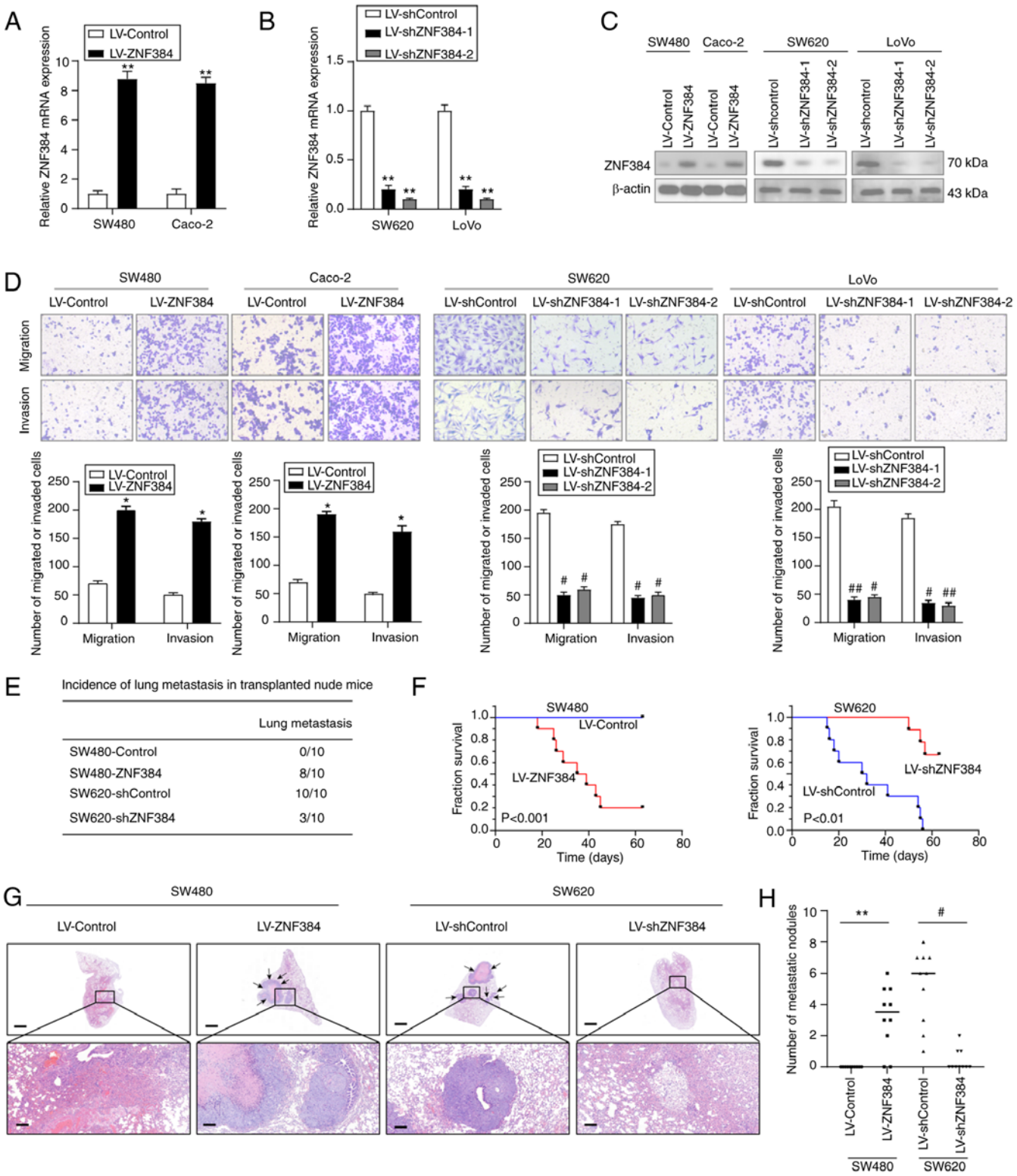

Figure 2. ZNF384 enhances CRC cell invasion and metastasis. (A-C) Reverse transcription-quantitative PCR and western blotting were carried out to verify ZNF384 overexpression in SW480 and Caco-2 cells, and ZNF384 knockdown in SW620 and LoVo cells. (A) **P<0.01 vs. LV-Control (B) **P<0.01 vs. LV-shControl. (D) Migration and invasion of CRC cells was detected using Transwell assays (magnification, x20). *P<0.05 vs. LV-Control; $^{\#}$P<0.05, $^{\#\#}$P<0.01 vs. LV-shControl (E) Number of mice with lung metastasis per group. (F) Overall survival outcomes for mice in every group. (G) Representative hematoxylin and eosin staining images showing lung metastases in mice injected with transfected cells via the tail vein. Scale bars, 1 mm (low magnification) and 100 μm (high magnification). (H) Numbers of lung metastatic nodules in various groups. **P<0.01 vs. LV-Control; $^{\#}$P<0.05 vs. LV-shControl. ZNF384, zinc finger protein 384; CRC, colorectal cancer; sh, short hairpin RNA.

hypoxia-mediated ZNF384 expression was involved in the transactivation of its promoter, a reporter plasmid with the ZNF384 gene promoter was transfected into CRC cell lines and subjected to hypoxia. Under conditions of hypoxia, ZNF384 transcription levels were markedly elevated, demonstrated by enhanced luciferase activities (Fig. 5C). HIF-1α

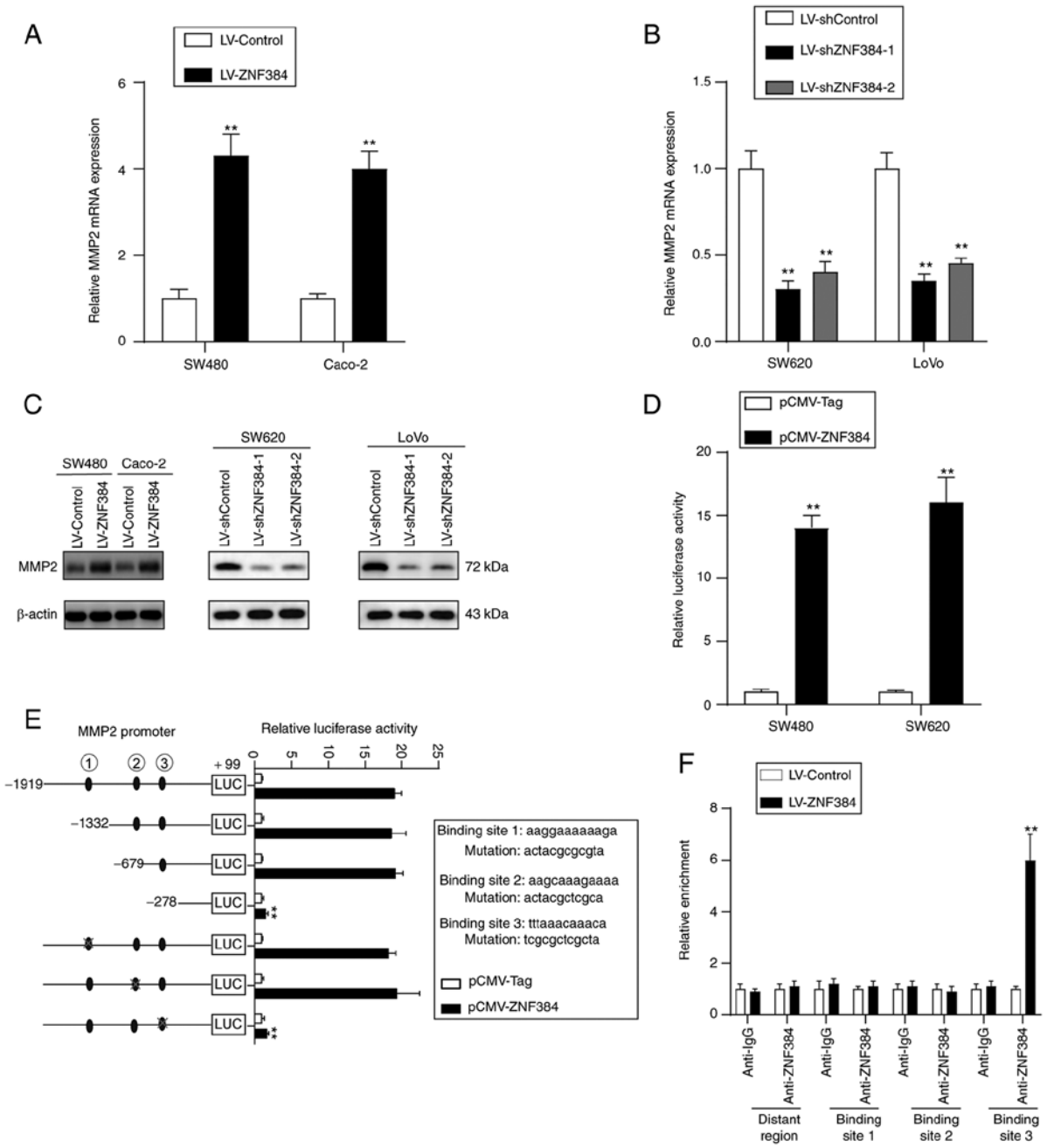

Figure 3. MMP2 is a direct transcriptional target of ZNF384. (A and B) MMP2 mRNA expression levels in CRC cells. (A) **P<0.01 vs. LV-Control; (B) **P<0.01 vs. LV-shControl. (C) Protein expression levels of MMP2 in CRC cells. (D) Luciferase activities of the reporter gene driven by the MMP2 promoter in CRC cells. **P<0.01 vs. pCMV-Tag (E) Luciferase activities of the reporter gene driven by the serially truncated/mutated MMP2 promoter indicates ZNF384 binding sites in SW480 cells. **P<0.01 vs. MMP2 promoter sequence (-1,919/+99). (F) Chromatin immunoprecipitation assay for the binding of ZNF384 to the MMP2 promoter in SW480 cells. Y-axis shows enrichment with anti-ZNF384 antibodies vs. the IgG control. **P<0.01 vs. anti-IgG. ZNF384, zinc finger protein 384; CRC, colorectal cancer; sh, short hairpin RNA.

overexpression was associated with high luciferase promoter activities, and elevated ZNF384 mRNA and protein expression levels, whereas HIF-1α knockdown exerted the opposite effects (Figs. 5D, S1M and N). Moreover, the ZNF384 promoter sequences were explored to establish potential cis-regulatory elements, and two putative HIF-1α-binding sites were identified through the JASPAR website. Site-directed mutagenesis and serial deletion assays revealed that both ZNF384-binding sites were crucial for HIF-1α-initiated ZNF384 transactivation (Fig. 5E). Results of the ChIP assay further verified the direct binding of HIF-1α to the ZNF384 promoter in CRC cells (Fig. 5F). The aforementioned findings demonstrated that ZNF384 is a target gene for HIF-1α.

ZNF384 expression is positively associated with HIF-1α and MMP2 expression levels in CRC. The potential association between ZNF384, MMP2 or HIF-1α expression in CRC tissues was evaluated. Results of the present study demonstrated that there was a positive association between ZNF384 and HIF-1α expression, and between ZNF384 and MMP2 expression (Fig. 6A and B), which was further verified using GEPIA (Fig. 6C).

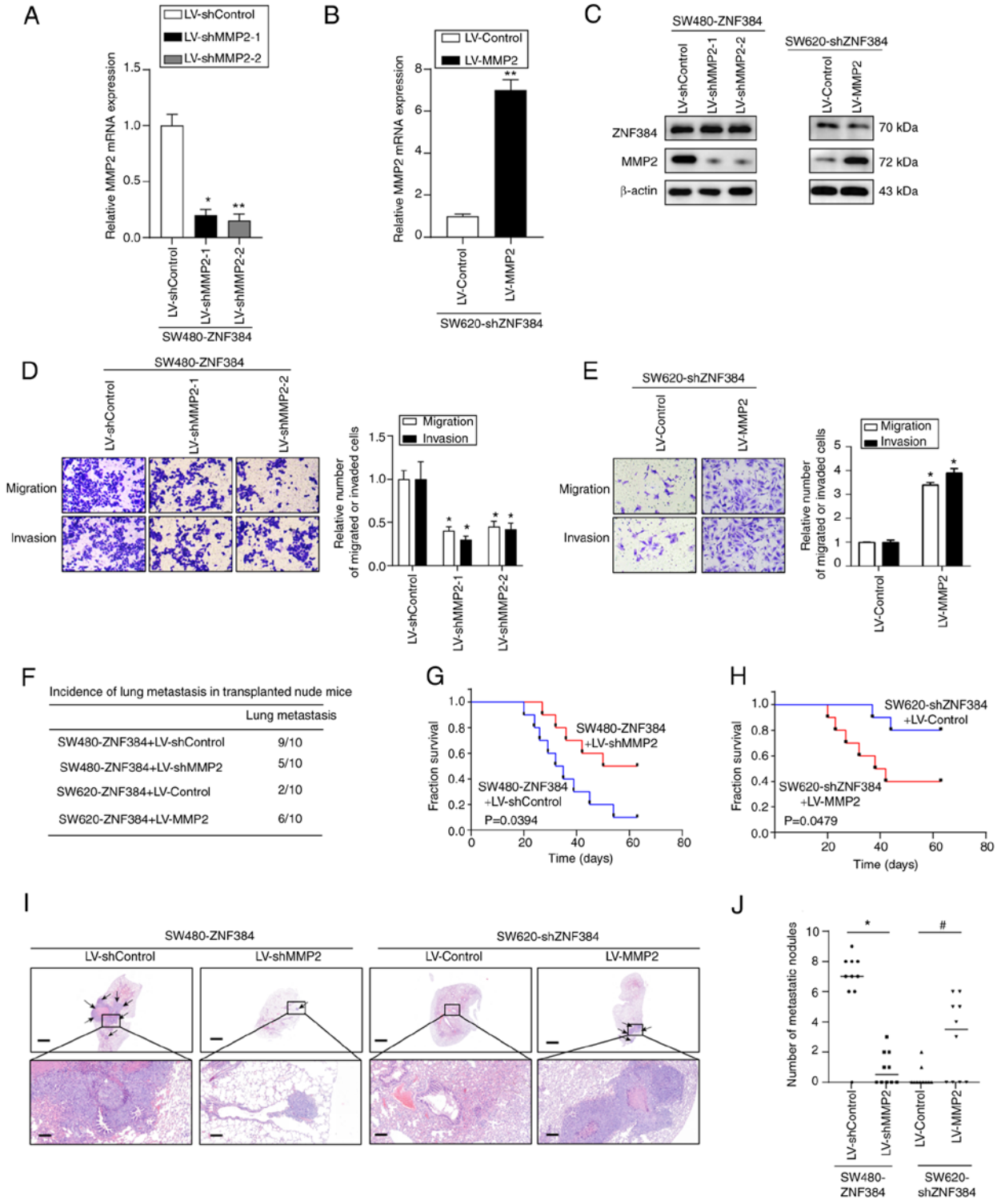

Figure 4. MMP2 is crucial for ZNF384-mediated CRC migration and metastasis. (A-C) Reverse transcription-quantitative PCR and western blotting were carried out to determine MMP2 expression in cells. (A) *P<0.05, **P<0.01 vs. LV-Control; (B) **P<0.01 vs. LV-shControl. (D and E) Transwell assays for indicated cells (magnification, x20). (D) *P<0.05 vs. LV-Control; (E) *P<0.05 vs. LV-shControl. (F) Number of mice per group with lung metastasis. (G and H) Overall survival outcomes of mice in each group. (I) Representative hematoxylin and eosin-stained lung tissue images. (J) Number of lung metastatic nodules in various groups. Scale bars, 1 mm (low magnification) and 100 μm (high magnification). *P<0.05 vs. LV-shControl; #P<0.05 vs. LV-Control. ZNF384, zinc finger protein 384; CRC, colorectal cancer; sh, short hairpin RNA.

Discussion

In numerous types of cancer, ZNF384 promotes various malignant processes, including cell proliferation, migration and invasion (9,27,28). Results of a previous study demonstrated that ZNF384 overexpression promoted melanoma cell progression (9). In addition, ZNF384 has been shown to bind the APOBEC3B (A3B) promoter to modulate A3B expression in cervical cancer (27). ZNF384 may also promote hepatocellular carcinoma (HCC) cell proliferation by promoting

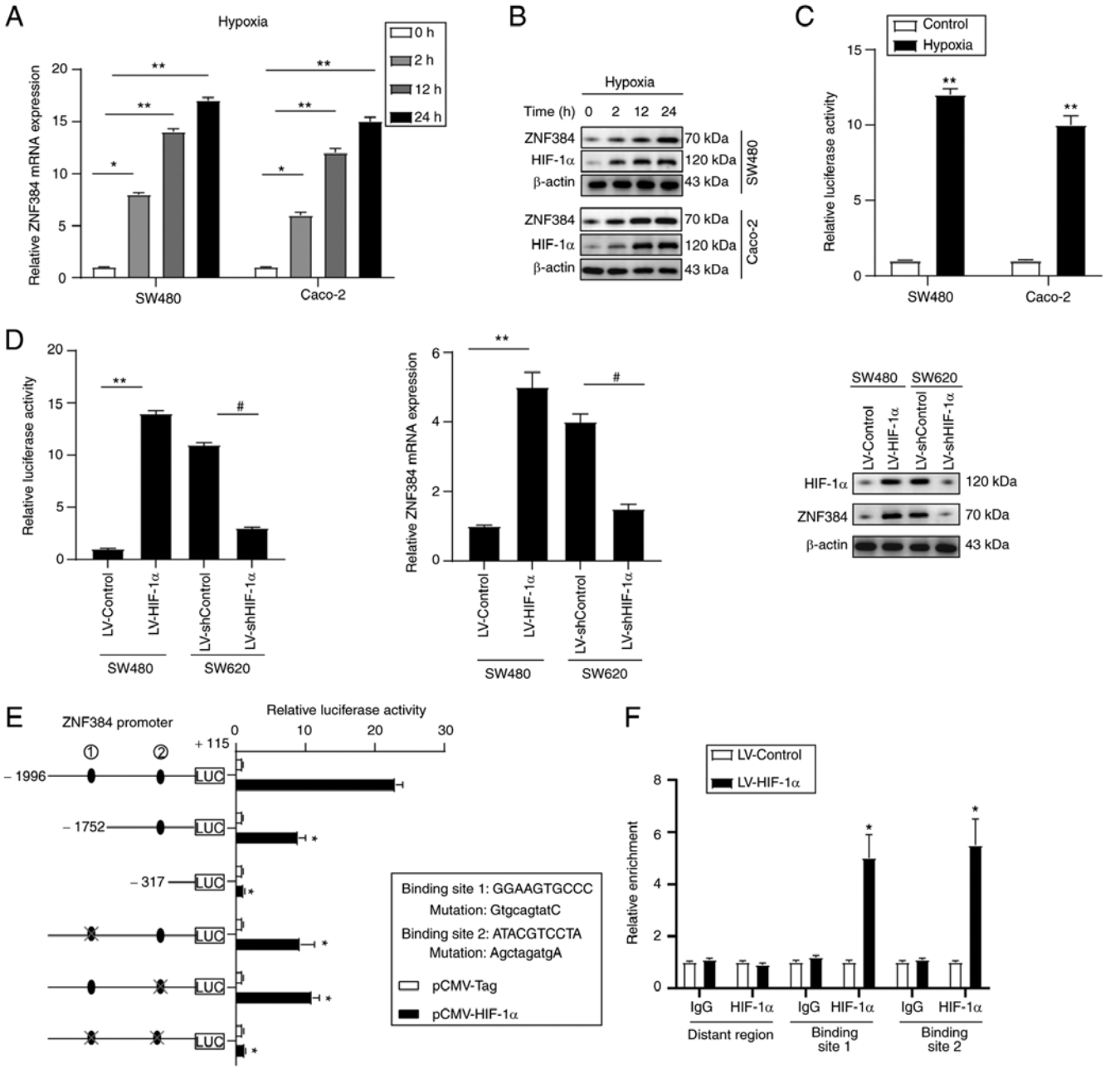

Figure 5. ZNF384 is a direct target gene for HIF-1α. CRC cells were cultured in a hypoxic atmosphere (0.5% O_2) for the indicated time intervals, after which ZNF384 expression was evaluated by (A) RT-qPCR and (B) western blot analysis. *P<0.05, **P<0.01 vs. 0 h. (C) Luciferase reporter construct with the (-1,996/+115) ZNF384 promoter was transfected in CRC cells, and luciferase activity was measured after 24 h. **P<0.01 vs. Control. (D) SW480 and SW620 cells were infected with LV-HIF-1α and LV-shHIF-1α. After 24 h, ZNF384 transcription and expression levels were assessed using luciferase assays (left panel), western blotting (right panel) and RT-qPCR (middle panel). **P<0.01 vs. LV-Control; $^{\#}$P<0.05 vs. LV-shControl. (E) Truncated and mutated ZNF384 promoter constructs were co-transfected with pCMV-HIF-1α in SW480 cells, after which relative luciferase activities were confirmed. *P<0.05 vs. ZNF384 promoter sequence (-1,996/+115). (F) Chromatin immunoprecipitation assays confirmed the binding of HIF-1α to the ZNF384 promoter in SW480 cells. *P<0.05 vs. anti-IgG. ZNF384, zinc finger protein 384; CRC, colorectal cancer; RT-qPCR, reverse transcription-quantitative PCR; HIF-1α, hypoxia-inducible factor 1α; sh, short hairpin RNA.

cyclin D1 expression and is considered a prognostic factor for patients with HCC (28).

The results of the present study demonstrated that ZNF384 was markedly elevated in metastatic CRC tissues, and increased ZNF384 expression was associated with lymph node metastasis and advanced clinical stage. ZNF384 expression was also revealed to be an independent risk factor for low patient survival outcomes following curative resection. Furthermore, the results of the present study demonstrated that ZNF384 overexpression markedly enhanced CRC metastasis, whereas ZNF384 knockdown exerted the opposite effects. However, the results of the present study revealed that ZNF384 expression did not affect CRC cell proliferation. The discrepancies in the function of ZNF384 in different types of cancer may be associated with differences in cellular context or differences in targeted genes. Therefore, in CRC, ZNF384 may act as a potential metastatic promoter and prognostic marker.

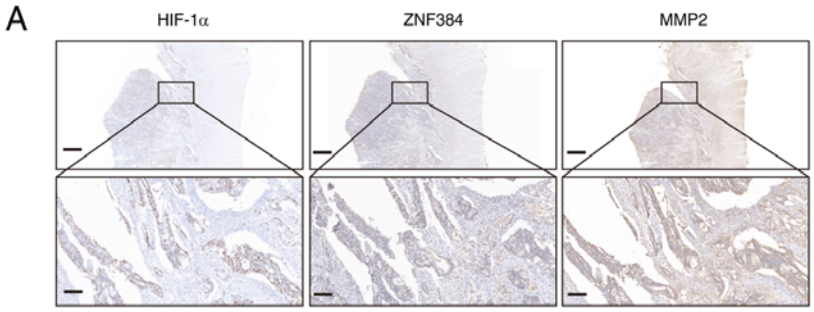

B Correlation analysis of ZNF384 expression and HIF-1α or MMP2 in 164 human CRC tissues

		ZNF384		
		Positive (n=66)	Negative (n=98)	
HIF-1α	Positive (n=97)	49	48	P=0.001
	Negative (n=67)	17	50	
MMP2	Positive (n=78)	41	37	P=0.002
	Negative (n=86)	25	61	

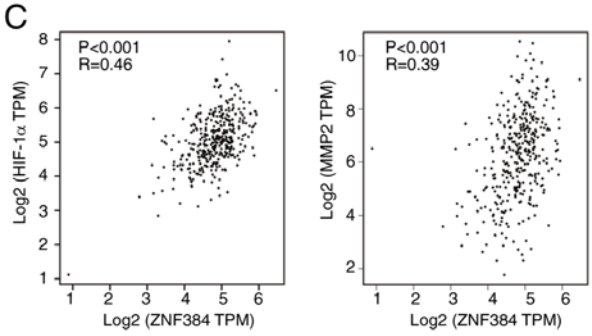

Figure 6. ZNF384 expression levels are positively correlated with MMP2 and HIF-1α expression levels in CRC. (A) Representative immunohistochemical staining images for ZNF384, HIF-1α and MMP2 in human CRC tissues. Scale bars, 200 μm (low magnification) and 50 μm (high magnification). (B) Association between ZNF384 expression levels, and HIF-1α and MMP2 expression levels in human CRC tissues. (C) Correlation between ZNF384 expression, and HIF-1α or MMP2 expression was analyzed by Gene Expression Profiling Interactive Analysis in colon or rectum adenocarcinoma. ZNF384, zinc finger protein 384; CRC, colorectal cancer; HIF-1α, hypoxia-inducible factor 1α.

MMPs are involved in cancer invasion and metastases (29). Among the MMPs, MMP2, also referred to as gelatinase A, plays critical roles in malignant cell migration, which is attributed to its ability to degrade type IV collagen (30). MMP2 is a potential prognostic biomarker (31). Elevated MMP2 expression in cancer cells has been reported to be a significant predictive factor for poor survival outcomes in CRC (31,32). Kostova *et al* (33) demonstrated a significant positive correlation between MMP2 tissue expression and the presence of nodal metastasis in CRC. Increased expression levels of MMP2 have also been shown to be correlated with poor overall and progression-free survival in patients with CRC (34). In CRC, increased levels of MMP2 have been revealed to be associated with microvascular angiogenesis and apoptotic resistance, and increased levels of MMP2 could elevate the levels of cell adhesion, and promote invasion and metastasis (35). The results of intrasplenic injection assays carried out in a previous study demonstrated that, in nude mice, the metastatic potential of CRC cell lines was associated with the levels of secreted MMP2 (36). These findings highlighted that MMP2 may be a crucial oncogene in CRC; however, the mechanisms through which MMP2 is dysregulated in CRC are yet to be fully elucidated. The results of the present study demonstrated that MMP2 was a direct functional target of ZNF384, which transactivates MMP2 expression by binding its promoter. Suppression of MMP2 markedly inhibited ZNF384-mediated CRC migration, invasion and lung metastasis, whereas MMP2 overexpression reversed the ZNF384 knockdown-induced suppression of CRC cell malignancy. Moreover, ZNF384 expression exhibited a positive correlation with MMP2 expression. In the present study, in addition to using serial deletion, site-directed mutagenesis was used as a control. Compared with the mutant plasmid, the wild-type plasmid had almost the same structure except the mutant base, which can also exclude the influence of nucleosomes. Therefore, these findings indicated that ZNF384 increased CRC metastasis by transactivating MMP2.

The mechanisms through which ZNF384 and MMP2 were dysregulated in CRC were also investigated. The association between hypoxia and MMPs, such as MMP2, has previously been verified (24). However, the role of hypoxia in ZNF384-associated MMP2 dysregulation has yet to be fully elucidated in human CRC. The results of the present study demonstrated two potential HIF-1α-binding sites in the ZNF384 promoter. Further analyses revealed that HIF-1α transactivated ZNF384 by binding both HIF-1α-binding sites within the ZNF384 promoter. Moreover, HIF-1α expression was correlated with ZNF384 expression levels. However, the results of the present study demonstrated that the trend in HIF-1α expression in CRC cells under conditions of normoxia were inconsistent with the expression levels of ZNF384 and MMP2. Thus, the ZNF384/MMP2 axis may not be regulated by HIF-1α under conditions of normoxia. Results of previous studies have demonstrated that hypoxia induces the Warburg effect, which is key in the development of cancer and may alter glucose metabolism (22,23). In the present study, the role of the HIF-1α/ZNF384/MMP2 axis in CRC progression has yet to be fully elucidated; thus, further investigations are required. The aforementioned results of the present study highlighted that the hypoxia-associated protein, HIF-1α, is a transcriptional regulator of ZNF384, which may enhance both MMP2 expression and CRC cell metastasis. These results highlight that under hypoxic conditions, human CRC progression may be promoted by dysregulated MMP2.

In conclusion, ZNF384, a direct HIF-1α target, was revealed to be markedly elevated in CRC and to be associated with poor prognostic outcomes. Furthermore, ZNF384 overexpression enhanced CRC cell metastasis by transactivating MMP2 expression. Therefore, these findings indicated that ZNF384 may act as a potential prognostic factor and therapeutic target for CRC.

Acknowledgments

Not applicable.

Funding

The present study was supported by the Sichuan Youth Science and Technology Foundation (grant no. 2017JQ0039).

Availability of data and materials

The datasets used and/or analyzed during the present study are available from the corresponding author on reasonable request.

Authors' contributions

ZY, YZ and YY designed the study, analyzed and interpreted the data, and wrote the manuscript. CZ analyzed and interpreted the data. PL and HT analyzed and interpreted the data, and wrote the manuscript. XT and GZ interpreted the data and confirm the authenticity of all the raw data. All authors read and approved the final manuscript.

Ethics approval and consent to participate

The present study was approved by the Medical Ethics Committee of North Sichuan Medical College [approval no. 2021ER(A)007]. All patients provided written informed consent for participation in the present study. The animal experiments were approved by the Experimental Animal Ethics Committee of North Sichuan Medical College (approval no. 20200908).

Patient consent for publication

Not applicable.

Competing interests

The authors declare that they have no competing interests.

References

1. Siegel RL, Miller KD and Jemal A: Cancer statistics, 2018. CA Cancer J Clin 68: 7-30, 2018.
2. Fakih MG: Metastatic colorectal cancer: Current state and future directions. J Clin Oncol 33: 1809-1824, 2015.
3. Punt CJ, Koopman M and Vermeulen L: From tumour heterogeneity to advances in precision treatment of colorectal cancer. Nat Rev Clin Oncol 14: 235-246, 2017.
4. Sato J, Nakamura M, Watanabe O, Yamamura T, Funasaka K, Ohno E, Miyahara R, Kawashima H, Goto H and Hirooka Y: Prospective study of factors important to achieve observation of the entire colon on colon capsule endoscopy. Therap Adv Gastroenterol 10: 20-31, 2017.
5. Nakamoto T, Yamagata T, Sakai R, Ogawa S, Honda H, Ueno H, Hirano N, Yazaki Y and Hirai H: CIZ, a zinc finger protein that interacts with p130(cas) and activates the expression of matrix metalloproteinases. Mol Cell Biol 20: 1649-1658, 2000.
6. Zhong CH, Prima V, Liang X, Frye C, McGavran L, Meltesen L, Wei Q, Boomer T, Varella-Garcia M, Gump J and Hunger SP: E2A-ZNF384 and NOL1-E2A fusion created by a cryptic t(12;19)(p13.3; p13.3) in acute leukemia. Leukemia 22: 723-729, 2008.
7. Do Amaral A: Complexities of nomenclature in biology. Gender of generic names ending in ops z, n, (s) 1572. Mem Inst Butantan 39: 27-36, 1975 (In Portuguese).
8. Lilljebjörn H and Fioretos T: New oncogenic subtypes in pediatric B-cell precursor acute lymphoblastic leukemia. Blood 130: 1395-1401, 2017.
9. Sakuma T, Nakamoto T, Hemmi H, Kitazawa S, Kitazawa R, Notomi T, Hayata T, Ezura Y, Amagasa T and Noda M: CIZ/NMP4 is expressed in B16 melanoma and forms a positive feedback loop with RANKL to promote migration of the melanoma cells. J Cell Physiol 227: 2807-2812, 2012.
10. Livak KJ and Schmittgen TD: Analysis of relative gene expression data using real-time quantitative PCR and the 2(-Delta Delta C(T)) method. Methods 25: 402-408, 2001.
11. Chandrashekar DS, Bashel B, Balasubramanya SAH, Creighton CJ, Ponce-Rodriguez I, Chakravarthi BVSK and Varambally S: UALCAN: A portal for facilitating tumor subgroup gene expression and survival analyses. Neoplasia 19: 649-658, 2017.
12. Tang Z, Kang B, Li C, Chen T and Zhang Z: GEPIA2: An enhanced web server for large-scale expression profiling and interactive analysis. Nucleic Acids Res 47: W556-W560, 2019.
13. Kent WJ, Sugnet CW, Furey TS, Roskin KM, Pringle TH, Zahler AM and Haussler D: The human genome browser at UCSC. Genome Res 12: 996-1006, 2002.
14. Castro-Mondragon JA, Riudavets-Puig R, Rauluseviciute I, Berhanu Lemma R, Turchi L, Blanc-Mathieu R, Lucas J, Boddie P, Khan A, Manosalva Pérez N, *et al*: JASPAR 2022: The 9th release of the open-access database of transcription factor binding profiles. Nucleic Acids Res 30: gkab1113, 2021.
15. Edge SB and Compton CC: The American Joint Committee on Cancer: The 7th edition of the AJCC cancer staging manual and the future of TNM. Ann Surg Oncol 17: 1471-1474, 2010.
16. Khemlina G, Ikeda S and Kurzrock R: The biology of Hepatocellular carcinoma: Implications for genomic and immune therapies. Mol Cancer 16: 149, 2017.
17. Fan Z, Tardif G, Hum D, Duval N, Pelletier JP and Martel-Pelletier J: Hsp90{beta} and p130(cas): Novel regulatory factors of MMP-13 expression in human osteoarthritic chondrocytes. Ann Rheum Dis 68: 976-982, 2009.
18. Torrungruang K, Alvarez M, Shah R, Onyia JE, Rhodes SJ and Bidwell JP: DNA binding and gene activation properties of the Nmp4 nuclear matrix transcription factors. J Biol Chem 277: 16153-16159, 2002.
19. Keith B, Johnson RS and Simon MC: HIF1α and HIF2α: Sibling rivalry in hypoxic tumour growth and progression. Nat Rev Cancer 12: 9-22, 2011.
20. Finger EC and Giaccia AJ: Hypoxia, inflammation, and the tumor microenvironment in metastatic disease. Cancer Metastasis Rev 29: 285-293, 2010.
21. Yoshimura H, Dhar DK, Kohno H, Kubota H, Fujii T, Ueda S, Kinugasa S, Tachibana M and Nagasue N: Prognostic impact of hypoxia-inducible factors 1alpha and 2alpha in colorectal cancer patients: Correlation with tumor angiogenesis and cyclooxygenase-2 expression. Clin Cancer Res 10: 8554-8560, 2004.
22. Renga G, Oikonomou V, Moretti S, Stincardini C, Bellet MM, Pariano M, Bartoli A, Brancorsini S, Mosci P, Finocchi A, *et al*: Thymosin β4 promotes autophagy and repair via HIF-1α stabilization in chronic granulomatous disease. Life Sci Alliance 2: e201900432, 2019.
23. Xu WL, Wang SH, Sun WB, Gao J, Ding XM, Kong J, Xu L and Ke S: Insufficient radiofrequency ablationinduced autophagy contributes to the rapid progression of residual hepatocellular carcinoma through the HIF-1α/BNIP3 signaling pathway. BMB Rep 52: 277-282, 2019.
24. Wang J, Ni Z, Duan Z, Wang G and Li F: Altered expression of hypoxia-inducible factor-1α (HIF-1α) and its regulatory genes in gastric cancer tissues. PLoS One 9: e99835, 2014.
25. Osinsky SP, Ganusevich II, Bubnovskaya LN, Valkovskaya NV, Kovelskaya AV, Sergienko TK and Zimina SV: Hypoxia level and matrix metalloproteinases-2 and -9 activity in Lewis lung carcinoma: Correlation with metastasis. Exp Oncol 27: 202-205, 2005.

26. Ryu J, Vicencio AG, Yeager ME, Kashgarian M, Haddad GG and Eickelberg O: Differential expression of matrix metalloproteinases and their inhibitors in human and mouse lung development. Thromb Haemost 94: 175-183, 2005.
27. Mori S, Takeuchi T, Ishii Y and Kukimoto I: Identification of APOBEC3B promoter elements responsible for activation by human papillomavirus type 16 E6. Biochem Biophys Res Commun 460: 555-560, 2015.
28. He L, Fan X, Li Y, Chen M, Cui B, Chen G, Dai Y, Zhou D, Hu X and Lin H: Overexpression of zinc finger protein 384 (ZNF 384), a poor prognostic predictor, promotes cell growth by upregulating the expression of Cyclin D1 in Hepatocellular carcinoma. Cell Death Dis 10: 444, 2019.
29. Shay G, Lynch CC and Fingleton B: Moving targets: Emerging roles for MMPs in cancer progression and metastasis. Matrix Biol 44-46: 200-206, 2015.
30. Nagase H and Woessner JF Jr: Matrix metalloproteinases. J Biol Chem 274: 21491-21494, 1999.
31. Zucker S and Vacirca J: Role of matrix metalloproteinases (MMPs) in colorectal cancer. Cancer Metastasis Rev 23: 101-117, 2004.
32. Leeman MF, Curran S and Murray GI: New insights into the roles of matrix metalloproteinases in colorectal cancer development and progression. J Pathol 201: 528-534, 2003.
33. Kostova E, Slaninka-Miceska M, Labacevski N, Jakovski K, Trojachanec J, Atanasovska E, Janevski V, Jovanovik R and Janevska V: Expression of matrix metalloproteinases 2, 7 and 9 in patients with colorectal cancer. Vojnosanit Pregl 71: 52-59, 2014.
34. Shi M, Yu B, Gao H, Mu J and Ji C: Matrix metalloproteinase 2 overexpression and prognosis in colorectal cancer: A meta-analysis. Mol Biol Rep 40: 617-623, 2013.
35. Egeblad M and Werb Z: New functions for the matrix metalloproteinases in cancer progression. Nat Rev Cancer 2: 161-174, 2002.
36. Shah V, Kumar S and Zirvi KA: Metastasis of human colon tumor cells in vivo: Correlation with the overexpression of plasminogen activators and 72 kDa gelatinase. In Vivo 8: 321-326, 1994.